

Enhanced Stability and Reusability of Subtilisin Carlsberg Through Immobilization on Magnetic Nanoparticles

Hassan Khan¹, Ihtisham Ul Haq²⁻⁴, Zahid Khan⁵, Muhammad Nughman¹, Zia Ur Rehman¹, Taj Ali Khan^{6,7}, Saadullah Khan¹, Mamdouh Allahyani⁸, Naif Alsiwiehri⁸, Mohammed A Alshamrani⁹, Aamir Shehzad¹⁰, Noor Muhammad¹

¹Department of Biotechnology & Genetic Engineering, Kohat University of Science & Technology, Kohat, Pakistan; ²Department of Physical Chemistry and Technology of Polymers, Silesian University of Technology, Gliwice, Poland; ³Joint Doctoral School, Silesian University of Technology, Gliwice, Poland; ⁴Programa de Pós-graduação em Inovação Tecnológica, Universidade Federal de Minas Gerais, Belo Horizonte, MG, Brazil; ⁵Institute of Chemical Sciences, University of Peshawar, Peshawar, Pakistan; ⁶Department of Pathology Khyber Teaching Hospital/Khyber Medical College Peshawar, Peshawar, Pakistan; ⁷Emerging Pathogens Institute, University of Florida, Gainesville, FL, USA; ⁸Department of Clinical Laboratory Science, College of Applied Medical Sciences, Taif University, Taif, Saudi Arabia; ⁹Department of Pharmaceutical Sciences, Pharmacy College, Umm Al-Qura University, Makkah, Saudi Arabia; ¹⁰Drug Discovery and Structural Biology Lab, Health Biotechnology Division, National Institute for Biotechnology and Genetic Engineering (NIBGE), Faisalabad, Pakistan

Correspondence: Noor Muhammad, Email dr.noor@kust.edu.pk

Introduction: Immobilizing enzymes on solid supports such as magnetic nanoparticles offers multi-dimensional advantages, including enhanced conformational, structural, and thermal stability for long-term storage and reusability.

Methodology: The gene encoding subtilisin Carlsberg was isolated from proteolytic *Bacillus haynesii*, a bacterium derived from salt mines. The nucleotide sequence encoding pro-peptide and mature protein were cloned into pET22(a)+ vector and expressed in *E. coli*. The extracted enzyme was subsequently immobilized on glutaraldehyde-linked-chitosan-coated magnetic nanoparticles.

Results: Fourier-transform infrared analysis revealed higher intensity peaks for the enzyme-immobilized nanoparticles indicating an increase in bonding numbers. X-ray diffraction analysis revealed a mild amorphous state for immobilized nanoparticles in contrast to a more crystalline state for free nanoparticles. An increased mass content and atomic percentage for carbon and nitrogen were recorded in EDX analysis for enzyme immobilized magnetic nanoparticles. Dynamic light scattering analysis showed an increase in average particle size from ~85 nm to ~250 nm. Upon enzyme immobilization, the Michaelis-Menten value increased from 11.5 mM to 15.02 mM, while the maximum velocity increased from 13 mm/min to 22.7 mm/min. Immobilization significantly improved the thermo-stability with 75% activity retained by immobilized enzyme at 70 °C compared to 50% activity by free enzyme at the same temperature. Immobilization yield, efficiency and activity recovery were 61%, 84% and 51%, respectively. The immobilized enzyme retained 70% of its activity after 10 cycles of reuse, and it maintained 55% of its activity compared to 50% activity by free enzyme after 30 days of storage.

Conclusion: The present study highlights the efficacy of magnetic nanoparticle-based immobilization in enhancing enzyme functioning and facilitates its incorporation into commercial applications necessitating high stability and reusability, including detergents, medicines, and bioremediation.

Keywords: enzymes, immobilization, nanoparticles, thermal stability, re-usability

Introduction

Enzymes serve as necessary biological catalysts that are critical for synthesis and breakdown reactions in all living organisms. In history, this role dates to ancient civilizations, although unknowingly, for processes like cheese making and wine production.¹⁻³ Recently, the industrial utilization of these catalysts has surged due to their capabilities to substitute the use of chemicals and other hazardous conditions like extremes of pH and temperature. These biological molecules have been considered eco-friendly for many years. Chemical pollutants, which are produced as a result of industrial

manufacturing processes, present a risk to both the environment and human health. Adoption of enzyme-based approaches for conversion reactions is considered as an environmentally sustainable strategy, with the potential to mitigate chemical pollutants.⁴⁻⁶ The catalytic abilities and diversified functionalities of enzymes are primarily attributed to microorganisms. However, essential constraints like low catalytic efficiency, activity, and stability under industrial environments have increased the need for novel strategies for their optimization. These strategies comprise the identification of microorganisms with spontaneously evolved enzymes suited for industrial tasks, engineering of the existing enzymes, and/or the immobilization of these catalysts to enhance their industrial applicability.^{4,6} One such microorganism that has been explored as a potential source of industrially relevant enzymes is *Bacillus haynesii*. *Bacillus haynesii* is a Gram-positive anaerobic bacterium initially isolated by Dunlap CA.⁷ This bacterium harbors genes for proteases, including subtilisin Carlsberg, in its genome. Subtilisins are a class of proteases that are categorized as serine proteases. These enzymes demonstrate activity at basic pH, featuring a serine residue at their active site for nucleophilic attack on peptide bonds.⁸ Serine alkaline proteases account for about 90% of all commercial enzymes sold annually, and they are widely used in industries such as food, detergent, and leather.⁹⁻¹¹ Subtilisins are involved in proteolytic activities for fulfilling the nutritional requirements of the bacteria and are secreted in the bacillus species. In the native subtilisin product, there is a (a) leading peptide – a guide for secretion, and (b) a pro-peptide – (chaperone) possibly for correct folding of the active part of the protein.^{12,13} Previously, subtilisin Carlsberg has been cloned in *Bacillus* species to obtain the product in the secreted form. *E. coli*, being a heterologous host for *Bacillus* genes, has not been used frequently for cloning of the subtilisin, however there are several studies where subtilisin genes from different bacillus species are cloned in *E. coli*, expressed, and confirmed for proteolytic activities.¹⁴ In 2016, Bjerga et al demonstrated the cloning of pro-peptide along with the active segment in *E. coli*, its cytoplasmic expression, and the activity of subtilisin Carlsberg.¹⁵ The native stability of subtilisins at alkaline pH restricts their industrial utilization, requiring engineered variants and immobilization of these enzymes on certain solid supports for practical applications.¹⁶

To address this limitation and enhance the stability and reusability of subtilisins, immobilization on novel matrices such as magnetic nanoparticles has emerged as a promising approach. Over the past decade, various enzymes have been immobilized on magnetic nanoparticles, demonstrating improved properties and extended applicability in industrial and biomedical processes.¹⁷ Such as lipases, widely used in the production of biodiesel and biopharmaceuticals, have been immobilized on functionalized magnetic nanoparticles, showing enhanced thermostability and activity in organic solvents.¹⁸ Similarly, amylases, crucial for starch processing industries, have exhibited improved catalytic efficiency and thermal stability upon immobilization on chitosan-coated magnetic nanoparticles.¹⁹ Proteases, like subtilisin and trypsin, have also been immobilized on magnetic supports for use in protein hydrolysis and detergent formulations. These systems often demonstrate improved reusability, making them economically viable for continuous processes.²⁰ In addition, glucose oxidase, a key enzyme in biosensors and food industries, has been immobilized on magnetic nanoparticles, significantly enhancing its operational stability and shelf life.²¹ Beyond industrial applications, peroxidases and catalases immobilized on magnetic nanoparticles have found use in environmental remediation, including wastewater treatment and the degradation of harmful pollutants. The immobilization of these oxidative enzymes enhances their durability and simplifies their recovery for repeated use.^{22,23}

Compared to conventional techniques, immobilization of enzymes on magnetic nanoparticles is a novel approach, safeguarding increased stability. Immobilization offers structural, conformational, and thermal stability, long-term storage capability, and reusability of enzymes, and, as a result, augments the overall enzymatic functionalities.²⁴ Enzyme immobilization can be achieved in several ways. Entrapment involves physically enclosing the enzyme within a porous matrix, such as alginate, agarose, or polyacrylamide gels. This method shields enzymes from external denaturation while allowing substrate diffusion into the matrix. However, entrapment often faces diffusional limitations, reducing reaction efficiency, particularly when working with larger substrates or viscous media.^{25,26} Encapsulation entails enclosing enzymes within a semi-permeable membrane or vesicle, such as liposomes or polymer microcapsules. This technique provides high protection against external conditions, ensuring the enzyme's structural integrity. However, encapsulation processes can be resource-intensive, and the membranes may hinder substrate access, potentially limiting activity.²⁷ Cross-Linking involves the creation of enzyme aggregates through chemical cross-linkers, such as glutaraldehyde. This method results in highly stable enzyme structures, often referred to as cross-linked enzyme aggregates

(CLEAs). Cross-linking enhances enzyme stability and prevents desorption but may lead to reduced catalytic efficiency if the enzyme's conformation is altered during the process.²⁸ Physical adsorption, one of the simplest immobilization methods, relies on non-covalent interactions, such as hydrophobic, ionic, or van der Waals forces, to attach enzymes to a support. While cost-effective and easy to implement, this method suffers from weak binding, making the enzyme prone to detachment under operational conditions.²⁹ For this purpose, covalent bonding is a commonly used approach. In this method, an enzyme and protein molecule's amino acids and a charged carrier surface that is insoluble in water form covalent bonds.^{30,31} The approach used presents some advantages such as the stability and strength of the covalent bond formed between the enzyme and the support surface preventing the dissociation of the enzyme and its leakage into the reaction mixture. In this case, the enzyme is bound to the surface of the support, which enhances its contact with the substrates. As a result, the strong engagement between the biocatalyst and the carrier leads to improved catalytic stability.³² Chitosan offers amino and hydroxyl groups in its structure that makes it an ideal carrier material for enzyme immobilization on solid surfaces. Glutaraldehyde is bifunctional reagents and can react with chitosan's amino groups to activate it by offering its second aldehyde group for binding with amino group of the concerned amino acid moiety on the surface of an enzyme.³³ Among various immobilization platforms, magnetic nanoparticles (MNPs) have gained attention due to their high surface area, ease of functionalization, and ability to be magnetically separated and reused. While several studies have explored the immobilization of different proteases on solid supports, limited attention has been directed toward the immobilization of subtilisin Carlsberg, a widely used serine protease known for its broad industrial applicability, including detergents, pharmaceuticals, and food processing.^{34,35} Previous studies on subtilisin immobilization have primarily focused on alternative supports such as silica-based materials, polymeric beads, or sol-gels, with limited structural or functional insights provided on enzyme performance post-immobilization.

This study involved the screening of protease-producing *Bacillus haynesii* obtained from a local salt mine in the Karak district of Khyber Pakhtunkhwa, Pakistan. The presence of the gene encoding a subtilisin-like serine protease was confirmed through PCR amplification and subsequent sequence analysis. Specific primers targeting the pro-peptide and native active regions of the gene segment were utilized for amplification, followed by cloning in *E. coli*. After expression and extraction, the obtained enzyme was immobilized on magnetic nanoparticles for improved catalytic activity, thermal stability, and enzyme recovery from the reaction mixture.

Methodology

Cloning and Expression of Subtilisin Carlsberg

The presence of the subtilisin Carlsberg gene was confirmed in *Bacillus haynesii* isolated from salt mines in district Karak, Pakistan, using degenerate primers (Table 1) for subtilisin-like serine proteases, followed by subsequent sequence analysis using the NCBI database. Restriction sites for NcoI and XhoI enzymes were incorporated at the ends of the amplified product. For expression of the target gene, pET28(a)+ expression vector was utilized, and the recombinant vector was introduced into competent *E. coli* BL21 Gold (DE3) cells.

Table 1 Primers Set Used for the Amplification of 16s rRNA and Subtilisin Gene

Primer	Forward	Reverse
Conserved sequence of 16s rRNA gene	27F AGAGTTTGATCCTGGCTCAG	1392R GGTTACCTTGTTACGACTT
Degenerate Primers for Subtilisin like protease	CAY GGI ACI CAY GTI GCI GG	CCI GCI ACR TGI GGI GTI GCC AT
Amplification of complete Sub-C gene	TCCTGTCAATTCGCGAACTCC	TCCTGTCAATTCGCGAACTCC
For Pro-peptide and Mature Sub-C	CTCAGCCGGCGAAAAAT	TTATTGAGCGGCAGCTTCG
For Pro-peptide and Mature Sub-C Forward Primer: (NcoI restriction site) Reverse Primer (XhoI restriction site)	CTccatggcaCTCAGCCGGCGAAAAAT	TTATTGAGCGGCAGCTTCGctcgagG

Production and Purification of the Enzyme

The transformed *E. coli* BL21 Gold (DE3) cells were initially cultured at 37 °C and 200 RPM for 14 hours. Upon reaching an OD of 0.6, 0.2 mM IPTG was used as inducer for target gene expression. The cells were then harvested at 4000 RPM, using a benchtop (Beckman Coulter) centrifuge at 4 °C for 20 minutes. The supernatant was removed, and the lysates were centrifuged at 5000 RPM for 15 minutes. The clear supernatant, representing the soluble fraction of the protein, was subjected to SDS-PAGE for the estimation of its molecular weight. The supernatant obtained was applied onto a His tag column (Complete His Tag, Roche) for affinity purification, and final elution was achieved using an imidazole buffer (250mM). Successful expression was confirmed through SDS-PAGE and a casein protease assay for enzyme activity.

Model Building and Structural Analysis for Identification of Target Residue for Immobilization

A three-dimensional (3D) model for the protease was calculated using the homology modelling approach. For this purpose, the MODELLER software (Wiederstein and Sippl 2007) was employed, and the known structure of subtilisin Carlsberg from *Bacillus licheniformis* (PDB code: 1SBC), having the highest sequence similarity with the target sequence, was used as a template. A total of 5 models were generated which were subsequently analyzed for the stereochemical quality using the PROCHECK program (Laskowski et al 1993) and energy profiles using the ProSA-web server (Wiederstein and Sippl 2007). The best model was selected for structural analysis. The model was visualized using the PyMOL Open tool (free available to download) (<http://www.pymol.org>).

Preparation of Magnetic Nanoparticles

For the preparation of magnetic Fe₃O₄ nanoparticles (Mag-NPs), a chemical co-precipitation method was employed as described by Saravanakumar et al (2014) with some modifications. A mixture of Fe²⁺ and Fe³⁺ ions in a 1:1 molar ratio was added to 25% (NH₄OH) solution, followed by vigorous stirring and heating at 65 °C for 15 minutes in a water bath. The magnetic nanoparticles (Mag-NPs) were extracted using an outer magnet.

Coating Chitosan on Magnetic Nanoparticles

For the preparation of chitosan-coated magnetic nanoparticles (Mag-CTS-NPs), magnetic nanoparticles (Mag-NPs) were dispersed in a 4 mg/mL chitosan suspension with the addition of a 0.5 mg/mL TPP (tripolyphosphate) solution simultaneously. This was followed by ultrasonic treatment at room temperature for 30 minutes.

Activation of (Mag-CTS-NPs) with Glutaraldehyde

To achieve the activation of Mag-CTS-NPs with glutaraldehyde, 50 mg of Mag-CTS-NPs were dispersed in 30 mL of 4% glutaraldehyde (GA) solution and stirring at 25 °C for 3–4 hours. The activated nanoparticles (Mag-CTS-GA-NPs) were then collected using an outer magnet (Nguyen et al 2019).

Functionalization of the Support Material (Mag-CTS-GA-NPs) with Enzyme

The Mag-CTS-GA-NPs (100mg) were activated and then suspended in a solution of 10 mL of 25 mM sodium phosphate buffer at pH 7.0. The solution also contained 18 U/mL of subtilisin activity in the presence of 0.01% cetrimonium bromide. The mixture was continuously stirred for 3 hours at a temperature of 25 °C. The immobilized subtilisin was then separated from the solution using magnetic decantation and washed with 25 mM sodium phosphate buffer.

Enzyme Activity Assay

For the estimation of enzyme activity, 0.6% casein solution was prepared in Tris-HCl buffer (pH 8.0), then 1 mL of the enzyme solution with activity of 18 U/mL and immobilized enzyme (Mag-CTS-GA-NPs) was added. This mixture was then incubated for 30 minutes at 40°C. After incubation, the mixture was centrifuged for 10 minutes, and absorbance was measured at 660 nm after adding 5 mL of 500 mM NaCO₃, followed by the addition of 1 mL of Folin & Ciocalteu

reagent. An enzyme activity unit (U) was defined as the amount of enzyme that releases 1 μmol of tyrosine per minute under optimal conditions.

Activity determining for the free enzyme, post-immobilization filtrate remaining, and the immobilized enzyme were determined using the above-mentioned procedure for each sample. Immobilization yield, efficiency, and activity recovery were calculated as described by.³⁶

pH and Temperature Optimization

Optimal pH and temperature for both the free and Mag-CTS-GA-Enz-NPs were determined by conducting reactions at a pH range of 7 to 11 by keeping all the other reaction conditions constant. Likewise, the effect of temperature on the activities of both the free and immobilized subtilisin Carlsberg was determined over a range of 40°C to 70°C.

Characterization of the Support and Enzyme Immobilized Support Material

Thermogravimetric analysis (TGA) was performed to determine the thermal decomposition properties of the Mag-NPs, Mag-CTS-GA-NPs and Mag-CTS-GA-Enz-NPs using Thermal Analyzer (STA 8000, Perkin Elmer USA). Fourier transform infra-red (FTIR Carry 630 Agilent Technologies USA) was used for determination of functional groups, X-ray diffraction patterns (XRD) was recorded on a rotating anode X-ray diffractometer, JDX-3532, JEOL, Japan at 40 kV, 30 mA with a CuK α ($\lambda=1.5418\text{\AA}$). Samples were scanned from 3° to 90° (2 θ) at a scanning rate of 3°/min. The three sample including (Mag-NPs, Mag-CTS-GA-NPs and Mag-CTS-GA-Enz-NPs) were analyzed using, EDX-7000 Shimadzu Japan for determination of elemental composition. Once the data was collected, the spectrum of the peaks was analyzed to identify the characteristic X-ray peaks corresponding to elements in the sample, and the height of the peak was analyzed for quantitative analysis of the sample. The determination of particle size distribution was conducted using dynamic light scattering (ZetaSizer Blue-Malvern Panalytical UK).

Enzyme Kinetics

The enzymatic activity of both the free enzyme and the enzyme immobilized on nanoparticles was assessed across a range of substrate concentrations (1–7 mM) under conditions of pH 10.0 and a temperature of 55 °C. The Lineweaver–Burk curve was generated by plotting the reciprocal of the reaction rate (1/V) against the reciprocal of the substrate concentration (1/[S]). The K_m and V_{max} values for both free and immobilized enzymes were obtained by calculating the slope and intercept of the resulting linear equation.

Results

Culturing and Identification of Bacterial Species

Halophilic bacteria were isolated in a salt medium as separate colonies. Isolated colonies were processed for the confirmation of proteolytic activities, and glycerol stocks were prepared. Clear zones of hydrolysis were observed after overnight incubation on skimmed milk agar plates ([Figure S1 supportive info](#)). The proteolytic strains were subjected to DNA isolation, and the extracted DNA was amplified using 16S rRNA gene universal primers through PCR ([Table 1](#)). The amplified PCR products were confirmed on 2% gel electrophoresis ([Figure S2 supportive info](#)). Sequence analysis through NCBI database confirmed the isolated bacteria as *Bacillus haynesii*, and the sequence was submitted to GenBank OM811293.1.

Cloning of the Target Gene (Subtilisin Carlsberg)

Degenerate primers were used for amplification of subtilisin-like proteases. Sequence analysis of the amplified product confirmed the presence of subtilisin gene in isolated strain of the *Bacillus haynesii*. Complete subtilisin gene was amplified using primer sequences, and sequence analysis showed 99% similarity with subtilisin Carlsberg.

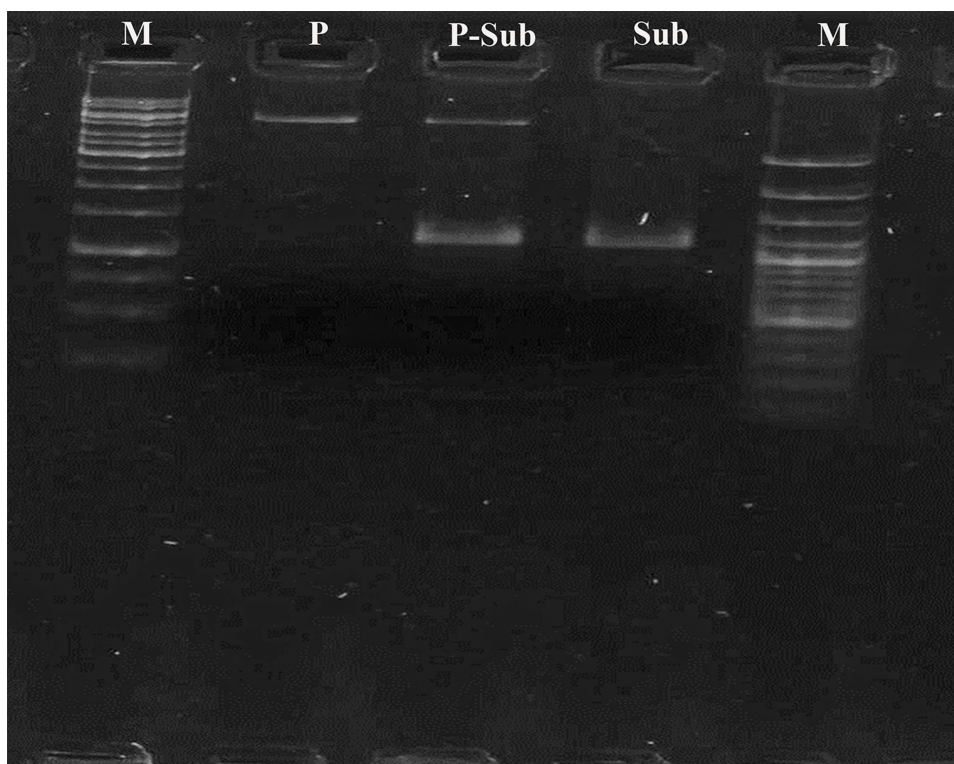


Figure 1 Confirmation of subtilisin Carlsberg and digested plasmid on agarose gel electrophoresis; Lane 1: marker, Lane 2: Plasmid, Lane 3: Subtilisin inserted plasmid, Lane 4: Subtilisin and Lane 5: Marker.

Cloning of Subtilisin Carlsberg Gene with Pro-Peptide Sequence

The pro-peptide and mature peptide without signal peptide were amplified using specific primers (Table 1), and the amplified product was cloned in pET28(a)+ vector and transferred into *E. coli*. Double digestion of the plasmid with NcoI and XhoI on agarose gel confirmed the cloning insert (Figure 1). Map of the transformed plasmid pET22 (a)+ vector, showing different region like promoter region, open reading frame and other genes. Different colour is used to highlight the different region and restriction sites, the colour indicate unique restriction sites of different enzymes (Figure S3 supportive info).

Optimal expression of the target gene was achieved by culturing the transformed *E. coli* cells at 37°C with shaking at 200 RPM and inducing expression with 0.2 mM isopropyl β -D-1-thiogalactopyranoside (IPTG) when the optical density (OD) reached 0.5–0.6.

Harvesting of Cells and Extraction of Protein

The cells were harvested for the isolation of protein, and SDS gel electrophoresis confirmed that the molecular weight of isolated protein was around 27 kDa (Figure S4 supportive info).

Structural Analysis for Immobilization of Subtilisin Carlsberg on Magnetic Nanoparticles

The structural analysis revealed that the subtilisin Carlsberg contains various polar amino acids, particularly serine and lysine, on its surface that could be targeted for immobilization of the protein on nanoparticles using a cross-linking agent. It is suggested that lysine residues are more suitable than serine residues for immobilization of the protease on nanoparticles due to the following reasons: i) unlike serine, lysine is not a catalytic residue of the protease, and any cross-linking reaction that involves lysine is, therefore, unlikely to negatively influence the catalytic activity of the enzyme, and ii) there are six lysine residues located on the surface of the enzyme that could be targeted for immobilization of the protease on nanoparticles (Figures S5–S8 Supportive info). In Figure 2, the predicted model in (green) and template

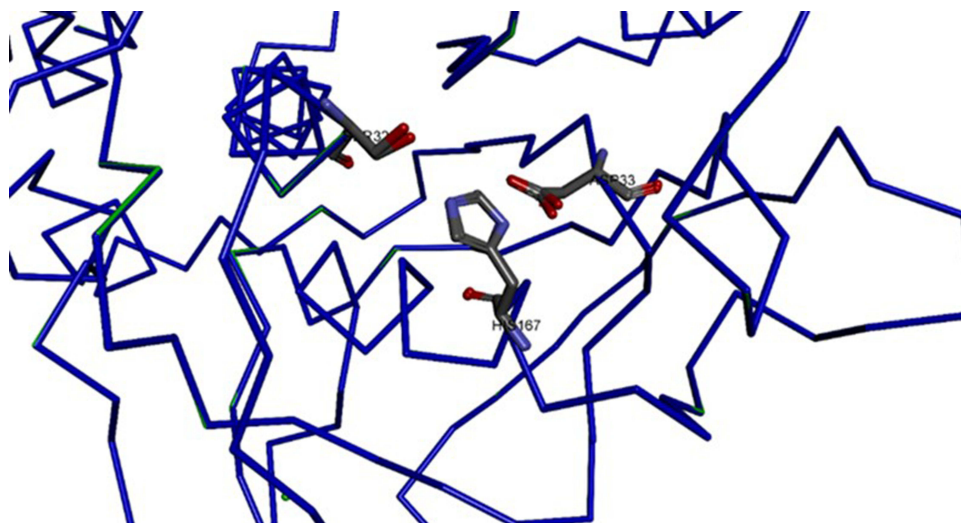


Figure 2 Structural model of the sequenced gene with Subtilisin Carlsberg (PDB code: ISBC) showing 97% similarity by superimposition of the two structures.

structures shown in (Blue) are superimposed. The active site residues (His, Thr, and Asp) have similar conserved conformations. Out of the 5 models generated using the MODELLER tool (Webb and Sali 2021), the best model contained more than 99.5% residues in the allowed regions, as indicated by the Ramachandran plot (Figure 3a). Furthermore, the best model has a ProSA energy score of -10 (Figure 3b), suggesting that the model could reliably be used as such for structural analysis without the need for performing energy minimization steps. The z-score of the predicted protein structure is -10 (as shown by the black dot), indicating a significant similarity to known experimental structures. This exceptionally low z-score suggests that the predicted conformation falls well within the acceptable range

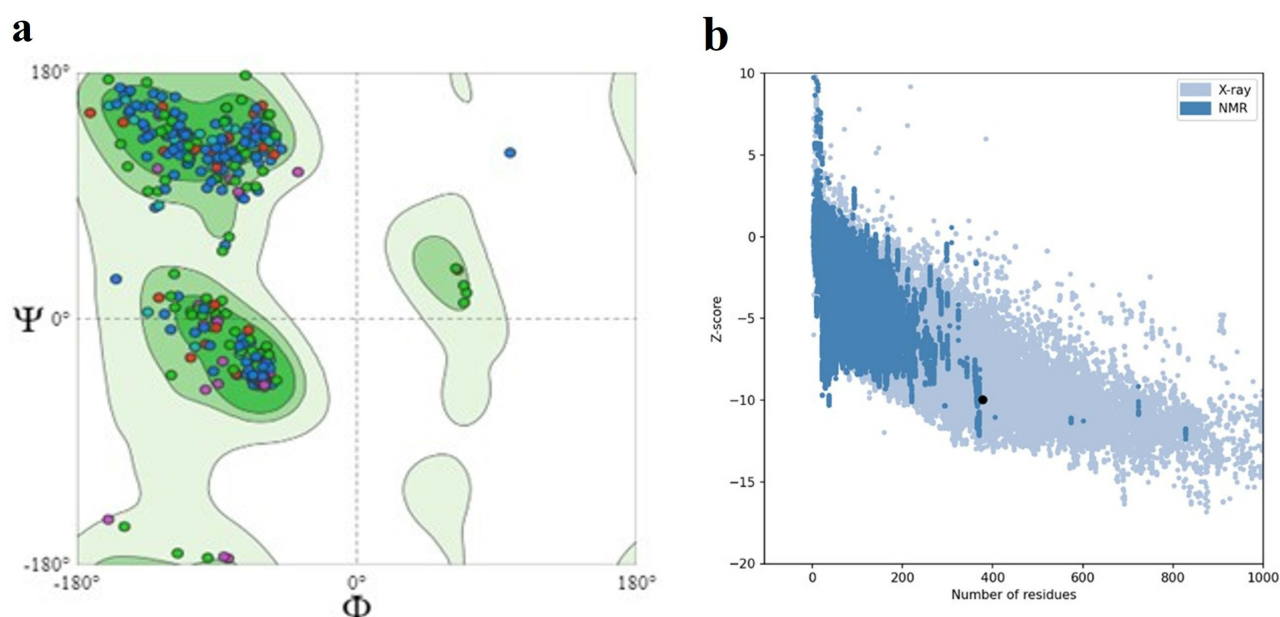


Figure 3 (a) The Ramachandran plot calculated using the PROCHECK program. The selected model contains 99.5% residues in the allowed regions (b) -score of the predicted model calculated using the ProSA-web server. The z-score of the predicted protein structure is -10 (as shown by the black dot) indicating a significant similarity to known experimental structures. This exceptionally low z-score suggests that the predicted conformation falls well within the acceptable range of structural variability. Structures with z-scores below 2 are typically considered to align closely with established conformations, and a z-score of -10 strongly supports the validity of this prediction.

of structural variability. Structures with z-scores below 2 are typically considered to align closely with established conformations, and a z-score of -10 strongly supports the validity of this prediction.

Analysis of Support Material and Enzyme Immobilized Support Material

Various physical and chemical analysis were performed for the characterization of the Mag-NPs, Mag-CTS-NPs, Mag-CTS-GA-NPs and Mag-CTS-GA-Enz ([Figures S4–S7 supportive info](#)).

FTIR Spectroscopy

FTIR spectroscopy confirmed the immobilization of Sub-C onto Mag-CTS-GA-NPs. The spectra of free nanoparticles (Mag-NPs), chitosan coated nanoparticles (Mag-CTS-NPs), glutaraldehyde activated chitosan coated nanoparticles (Mag-CTS-GA-NPs), and enzyme-immobilized nanoparticles (Mag-CTS-GA-Enz-NPs) are shown in [Figure 4](#). A detectable shift in the peaks around 3130.9 cm^{-1} , 2359.4 cm^{-1} , 2117.1 cm^{-1} , 1643.7 and 1054.8 suggests the pattern of distinct change in frequencies.

XRD Analysis

X-ray diffraction of materials determines the crystal structure, composition, and orientation of materials by assessing how X-rays deflect off their atoms. XRD patterns of the free nanoparticles (Mag-NPs), chitosan-coated nanoparticles (Mag-CTS-NPs), glutaraldehyde-activated chitosan-coated nanoparticles (Mag-CTS-GA-NPs), and enzyme-immobilized nanoparticles (Mag-CTS-GA-Enz-NPs) are shown in [Figure 5](#). In all the four samples, there is a display of six characteristic peaks for Fe_3O_4 . These peaks, identified by their indices (220), (311), (400), (422), (511), and (440) at 2θ angles of 30.1 ,

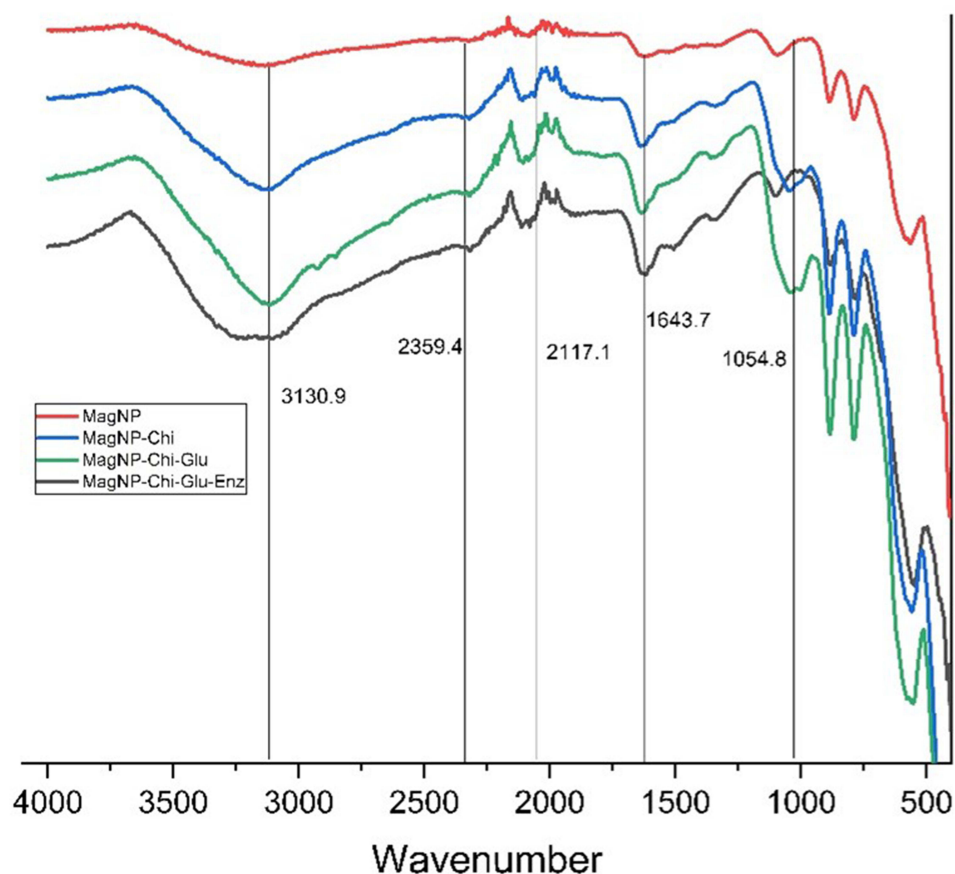


Figure 4 Fourier Transform Infrared (FTIR) spectra of Free Mag-NP (red), Mag-NP-Chi (blue), Mag-NP-Chi-Glu (green) and Mag-NP-Chi-Glu-Enz (black).

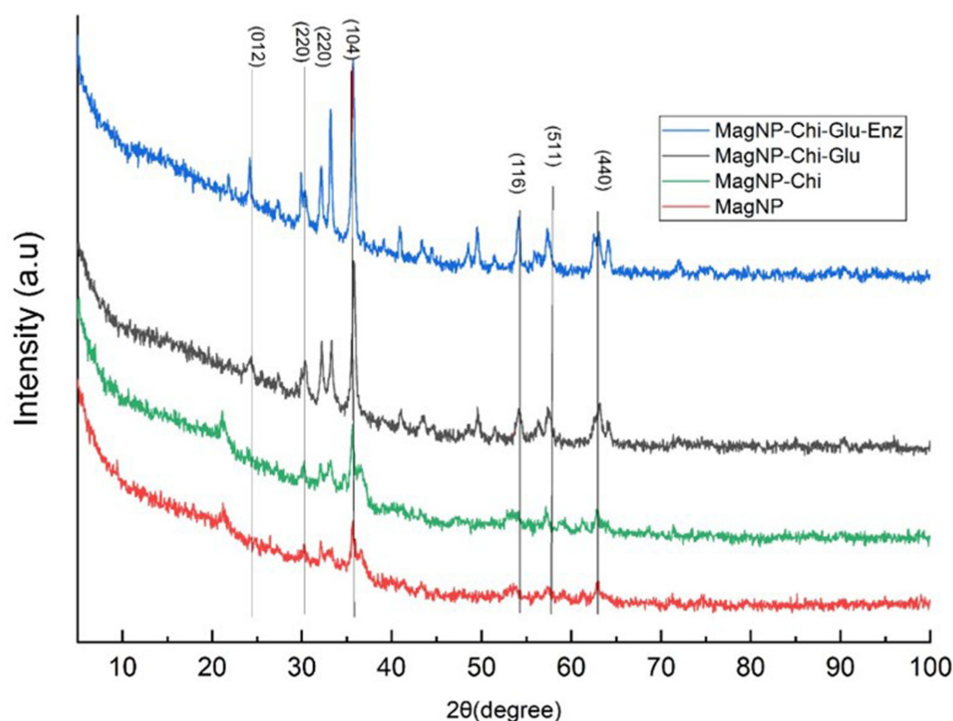


Figure 5 XRD pattern of Free Mag-NP (red), Mag-NP-Chi (green), Mag-NP-Chi-Glu (black), MagNP-Chi-Glu-Enz (blue).

35.5, 43.1, 53.4, 57.0, and 62.6 degrees, were nearly consistent for all samples. The binding of enzyme did not induce any major phase changes of Fe_3O_4 .

Dynamic Light Scattering (DLS)

Our results indicate that free Fe_3O_4 nanoparticles have an average size of approximately 80 nm [Figure 6a](#). Mag-NPs with enzyme indicate average size of approximately 250 nm [Figure 6b](#). Mag-CTS-NPs show an average size of approximately 90 nm [Figure 6c](#). Mag-CTS-GA-NPs indicate an average size of approximately 150 nm [Figure 6d](#).

TGA Analysis

The thermal degradation trends were examined between 100 and 800 °C for three samples. [Figure 7](#) displays the weight loss curves for immobilized enzyme Mag-CTS-GA-Enz and CTS-GA coated and uncoated Mag-NPs. In the temperature range of 125–750 °C. From the weight loss profile, it can be observed that free nanoparticle lost 7% of its weight at 750 °C, in contrast to enzyme immobilized Mag-NPs which lost almost 30% of its weight at the same temperature. The TGA profile of the immobilized nanoparticles exhibited three distinct stages of weight loss, corresponding to water loss, thermal degradation of the organic matrix, and eventual decomposition of residual organic material. The initial weight loss, occurring between 100°C and 150°C, was attributed to the loss of adsorbed and bound water molecules. This step was more pronounced in the immobilized nanoparticles due to the hydrophilic nature of the enzyme and the chitosan coating, both of which enhance water retention. The second stage of weight loss, occurring between 500°C and 600°C, corresponded to the thermal degradation of the chitosan coating and the enzyme. The decomposition of chitosan is likely initiated at around 580 °C, while the enzyme contributed to further weight loss at slightly higher temperatures. This trend supports successful immobilization, as the observed weight loss in this temperature range, was significantly higher than that of the bare nanoparticles, which lacked an organic matrix. The third and final stage, above 580 °C, was associated with the decomposition of remaining organic residues, including residual enzyme fragments and cross-linking agents such as glutaraldehyde. The reduced residue weight at this stage, compared to bare nanoparticles, indicated the effective decomposition of organic components associated with immobilization.

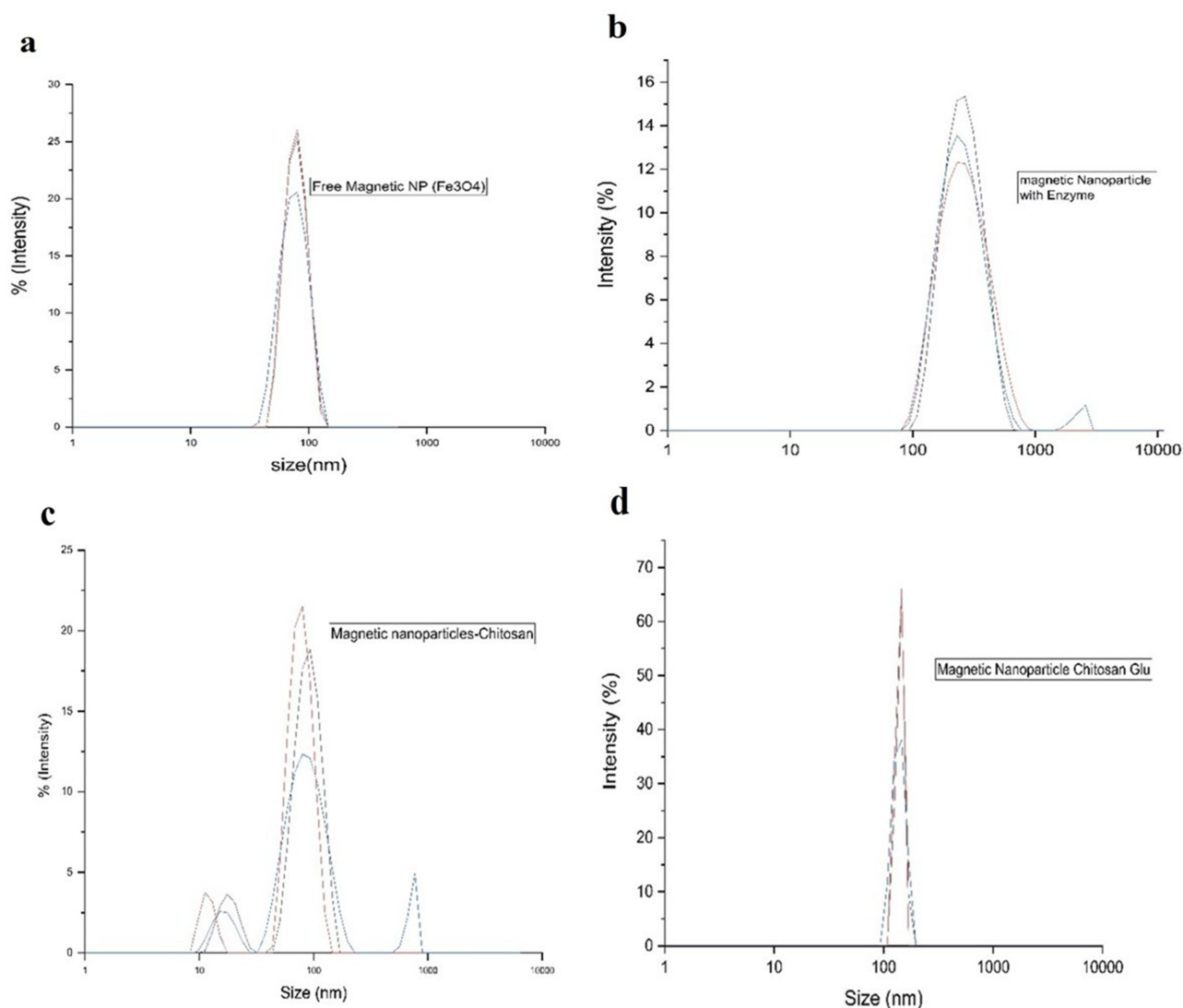


Figure 6 DLS of size distribution particles: (a) DLS of Free Mag-NP (b) DLS of Enzyme attached nanoparticles (c) DLS of MagNP-Chi (d) MagNP-Chi-Glu.

EDX Analysis

In the case of the enzyme immobilized magnetic nanoparticles (Mag-CTS-GA-Enz), the EDX analysis showed an increase in the intensity of the peaks that are corresponding to carbon (C) and nitrogen (N) and was markedly higher compared to the (Mag-CTS-GA-NPs). The increase in the elemental composition for carbon (C) and nitrogen (N) in the enzyme immobilized nanoparticles clearly signifies the presence and inclusion of these elements within the sample, indicating a successful immobilization of the enzyme as shown in the Figure 8a–c.

Enzyme Kinetics

To determine initial velocities for kinetic parameters, reactions were conducted at various casein concentrations ranging from (1–7 mM) for 15 minutes. The Michaelis–Menten constants (K_m) and (V_{max}) values of both the free enzyme and (Mag-NPs) immobilized enzymes were found by analyzing the Lineweaver-Burk graphs through non-linear curve fitting. The immobilization process resulted in an increase in the K_m constant from 11.5 mM to 15.02 mM. In this case, V_{max} increased from 13 to 22.7, which can be attributed to an increase in the enzyme stability and altered microenvironment of the enzyme (Figure 9).

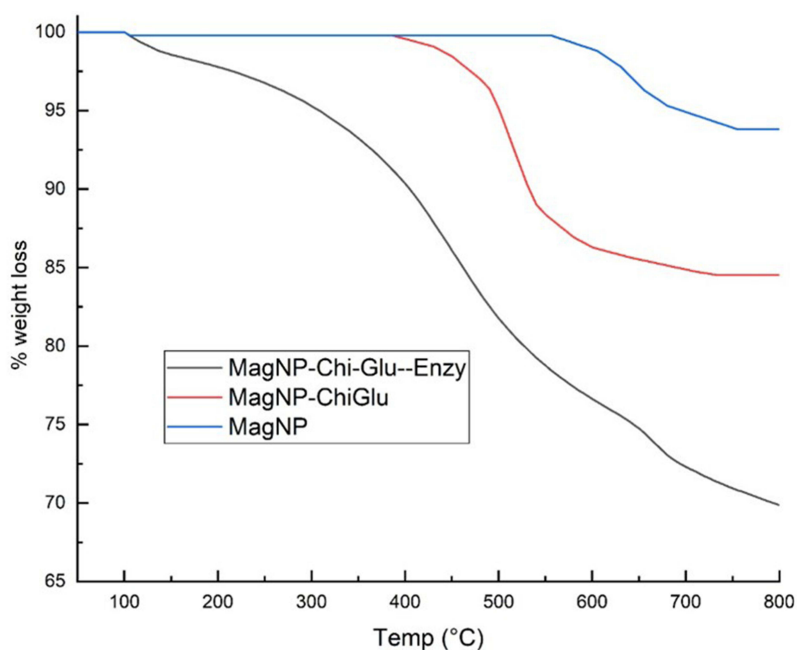


Figure 7 Thermogravimetric analysis of Mag-NP (blue), Mag-NP-Chi-Glu (red), and MagNP-Chi-Glu-Enzy (black).

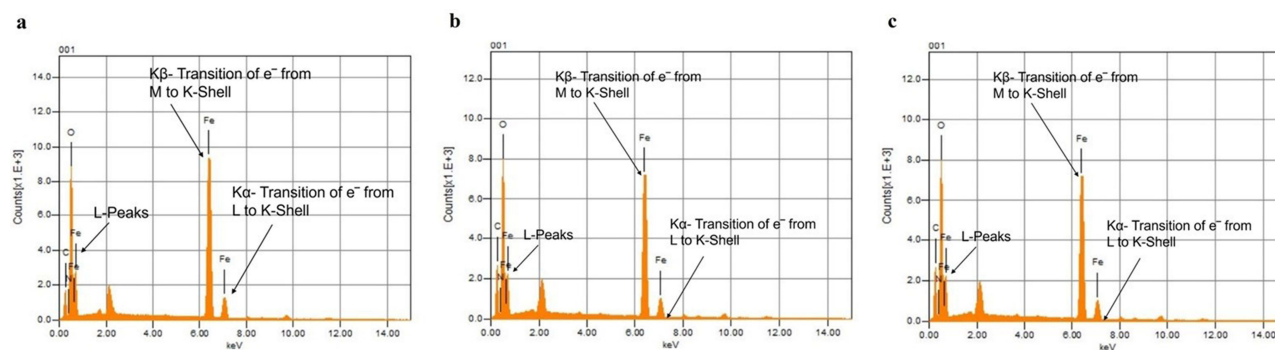


Figure 8 EDX analysis (a) magnetic nanoparticles (Mag-NPs), (b) (Mag-CTS-GA-NPs), (c) magnetic nanoparticles (Mag-CTS-GA-Enz-NPs).

Immobilization Yield, Efficiency, and Activity Recovery

The determination of immobilized enzyme activity involves calculating the difference between the initial enzyme activity and the remaining enzyme activity in the enzyme solution after immobilization. The initial step involves utilizing subtilisin Carlsberg as the catalyst in the immobilization mixture.

$$\text{Immobilization Yield (\%)} = 100 \times (\text{observed activity} / \text{starting activity of total free enzyme})$$

Immobilization efficiency describes the percent activity of the enzyme that is found in the immobilized state.

$$\text{Efficiency (\%)} = 100 \times (\text{immobilized activity} / \text{Starting activity})$$

Observed activity is measured by calculating the actual activity of the immobilized enzyme. In this case, the activity of Mag-CTS-GA-Enz-NPs is the observed activity. The third parameter frequently employed to assess the success of immobilization is the activity recovery. This is obtained by multiplying immobilization yield with immobilization efficiency. Activity recovery is to represent the percentage of observed activity in comparison to the starting activity.

$$\text{Activity recovery (\%)} = 100 \times (\text{observed activity of immobilized enzyme} / \text{starting activity of free enzyme})$$

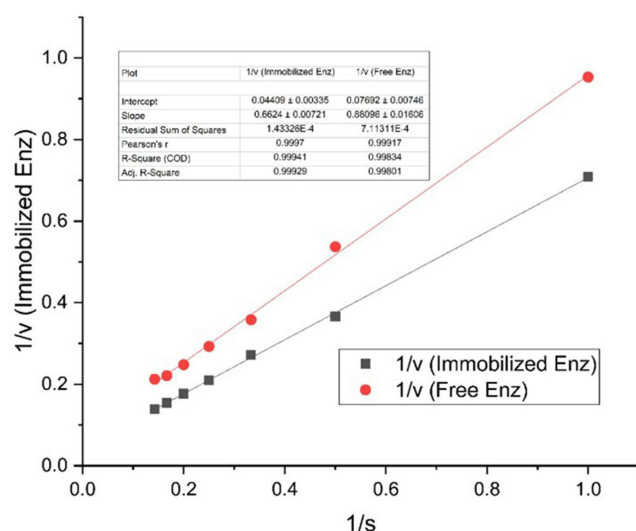


Figure 9 Lineweaver-Burk plots for kinetic parameters determination of free enzymes and immobilized enzymes.

The data shown in Table 2 reveals that about 61% of the enzyme activity in the solution becomes immobilized onto the magnetic nanoparticles. The observed efficiency is approximately 84%. The total activity recovery in this case is about 50%. Post-immobilization decline in enzyme activity is attributed to conformational alterations that usually happen during the covalent binding of the enzyme to the carrier.

Stability Studies of Immobilized and Free Enzyme

Enzymes covalently attached to support usually lose some activity, however it notably enhances the enzyme's thermal stability in comparison to its free form in the solution. Our results in (Figure 9) indicate that the free enzyme shows 90% activity at 55 °C while immobilized enzyme shows 95% activity at 55 °C. At 60 °C, the immobilized enzyme retains 80% activity. Overall, the thermal stability analysis of free and immobilized enzymes across temperatures from 40 °C to 70 °C reveals that the free enzyme retains up to 55% activity with the rise of temperature, while immobilized enzymes can retain up to 75% activity (Figure 10).

Optimum pH for Free and Immobilized Enzyme

In this study, various pH conditions ranging from pH 7.0 to 11 were used to assess the effect of pH change on free subtilisin Carlsberg and immobilized subtilisin Carlsberg using casein as a substrate. The results are displayed in Figure 11, showing the relative activity of both the free and immobilized subtilisin Carlsberg. The results of our study suggest that the most favorable pH for the free enzyme is 10, but the most favorable pH for the immobilized enzyme is 9.5. The optimal pH for both the free and immobilized enzyme remained fairly constant, with a pH difference of only 0.5.

Table 2 Immobilization Yield, Efficiency, and Activity Recovery of Enzyme on Magnetic Nanoparticles

Parameter	Value (%)
Immobilization Yield	61
Immobilization Efficiency	84
Activity Recovery	50

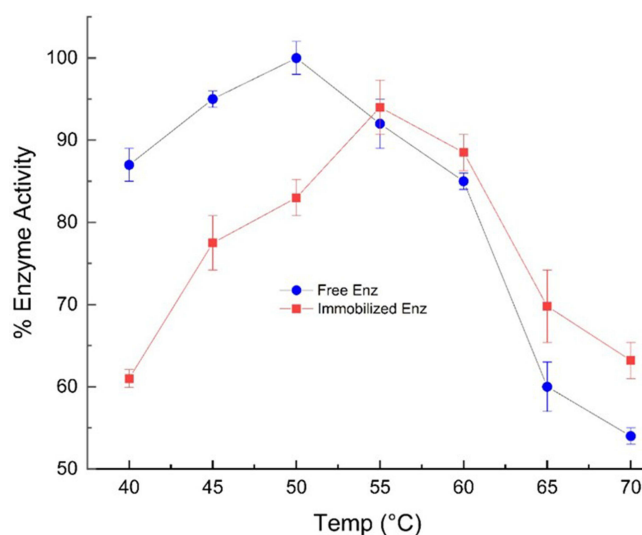


Figure 10 Effect of temperature on percent activity of the enzyme; Free Enzyme (blue), Immobilized Enzyme (red).

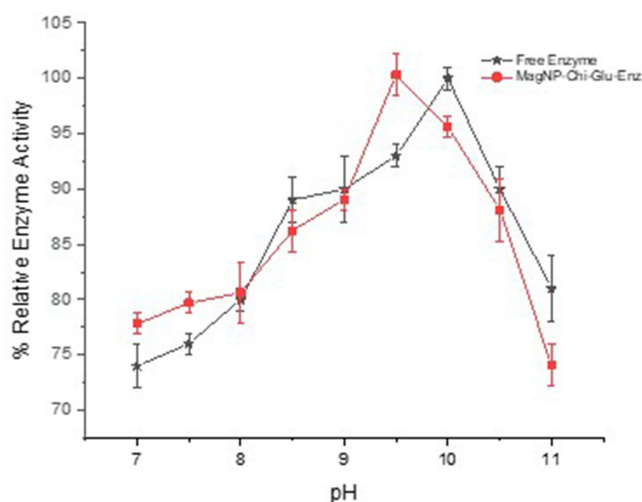


Figure 11 Effect of pH on percent activity of the enzyme; Free Enzyme (black), Immobilized Enzyme (red).

The immobilized enzyme exhibits greater activity than the free enzyme between pH 7.0 and 7.5. At pH 10.5 immobilized enzyme has about 85% activity while free enzyme has 90% activity.

Storage and Reusability Experiments

Both free and immobilized enzymes were stored at 4 °C, and their activities were detected for a period of 30 days at 3-day intervals. Figure 12 shows the percentage relative activities, with the starting activity of the two samples set at 100% activity. The activity graph indicates that after 15 days of storage, the free enzyme exhibited around 70% activity, while the magnetic nanoparticle-immobilized enzyme retained 75% activity. The same 75% percent activity level was persistent in the immobilized enzyme until the 21st day of storage.

By day 25, the activity of the free enzyme decreased to nearly 50%, while the immobilized enzyme retained around 65% activity. On day 30, the activity of the free enzyme dropped below 50%, whereas the immobilized enzyme showed approximately 53% activity. Figure 13 illustrates the enzyme activity of the immobilized enzyme at various cycles. It was noted that the immobilized enzyme maintained 70% of its activity across 10 cycles.

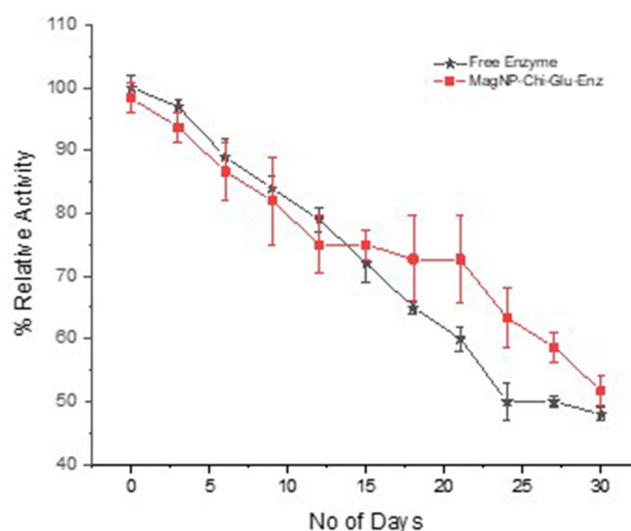


Figure 12 Effect of immobilization on storage stability. Free enzyme (black) Immobilized enzyme (red).

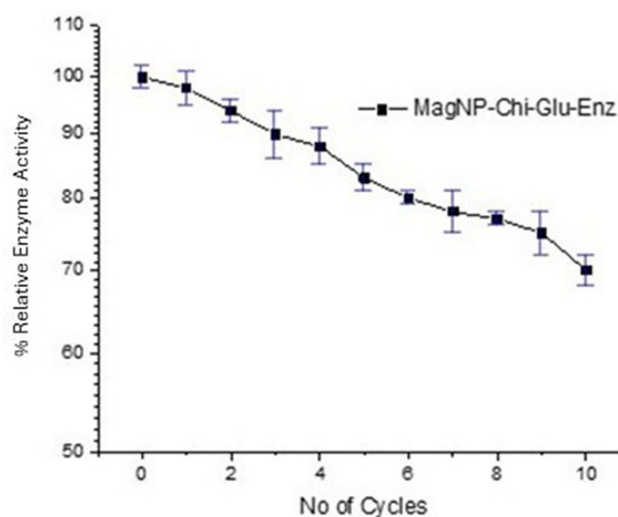


Figure 13 Reusability of immobilized enzyme over multiple cycles.

Discussion

The present study focusses on isolating halophilic bacteria that are able to produce industrially important enzymes (proteases). For this purpose, the salt mines of Karak (Pakistan) were screened for the isolation of proteolytic bacteria, which resulted in the isolation of proteolytic *Bacillus haynesii*. Bacteria from different extreme environments have gained significant attention because of exceptional adaptation and the ability to produce different enzymes having strong catalytic properties and enhanced stability.^{37,38} The production of protease enzymes by the isolated bacteria was detected by observing clear zones surrounding the bacterial colonies grown on skim milk agar media. The proteolytic bacteria were then identified using 16S rRNA gene through PCR amplification. These results show the significance of extreme environments, such as salt mines in this case, for the isolation of bacteria that naturally produce industrially important enzymes.^{39,40} The heterologous expression of subtilisin Carlsberg gene in *E. coli* signifies an important step for the production and characterization of these important enzymes. Subtilisin is a serine protease, having widespread applications in leather, detergent, and food processing, because of high catalytic efficiency and stability under various harsh conditions such as alkaline pH and higher temperature.^{36,41} The subtilisin gene was successfully amplified using degenerate primers and subsequently cloned in pET28(a)+ vector, which shows the importance of molecular cloning

in the isolation and expression of desired genes from diverse microbial communities.^{16,42} The use of inducers such as IPTG and the optimization of the expression is very important for maximizing the yield of recombinant enzymes.⁴³ The expression of the subtilisin Carlsberg was further validated through the estimation of its molecular weight using SDS-PAGE analysis.⁴⁴ The predicted structural model of subtilisin Carlsberg showed a high degree of similarity between the enzyme's active site residues (His, Thr, and Asp) and those in the template structure, confirming the conservation of key catalytic sites. The MODELLER tool⁴⁵ generated five models, with the best model demonstrating exceptional structural integrity. More than 99.5% of the residues in the best model were found within the allowed regions according to the Ramachandran plot (Figure 3a), indicating high-quality modeling. Additionally, the ProSA energy score of -10 (Figure 3b) further supports the reliability of the model, suggesting that it is energetically stable and suitable for structural analysis without the need for further energy minimization.⁴⁶

Enzymes being attached to solid supports, like magnetic nanoparticles, have become a viable method to improve their stability, capacity to be used several times, and overall effectiveness in catalyzing reactions.^{47,48} In this study, the subtilisin Carlsberg enzyme was immobilized onto glutaraldehyde-linked chitosan-coated magnetic nanoparticles (Mag-CTS-GA-NPs). The immobilization of subtilisin Carlsberg on magnetic nanoparticles using glutaraldehyde-linked chitosan offers several advantages in terms of stability and reusability as compared to other alternative immobilization strategies such as physical adsorption, entrapment in polymer matrices, and covalent bonding to non-magnetic carriers.⁴⁹ Physical adsorption methods, while cost-effective and simple, often result in weak enzyme-support interactions, leading to poor stability during repetitive use or under extreme conditions.⁵⁰ Entrapment in polymer matrices can provide protection to enzymes but may restrict substrate access, resulting in lower catalytic efficiency.²⁹ For instance, prior studies on subtilisin immobilization via alginate entrapment demonstrated reduced V_{max} values compared to the free enzyme, likely due to diffusional limitations.⁵¹ Covalent bonding to non-magnetic carriers, such as silica or polystyrene beads, provides stability but lacks the ease of separation offered by magnetic carriers, which is a distinct advantage in industrial processes.⁵² The use of magnetic nanoparticles, which allow efficient separation of the immobilized enzyme from reaction mixtures through magnetic fields, a feature readily adaptable to large-scale processes. Magnetic separation reduces the need for high-speed centrifugation or filtration, thereby lowering operational costs and energy requirements in scaled-up systems.⁵³

Before immobilization a prediction for amino acid residue on the outer part of enzyme molecule was needed that could potentially take part in binding with the carbonyl group of glutaraldehyde. Therefore, based on the sequence obtained for subtilisin Carlsberg from *Bacillus haynesii*, a model was developed using a Modeler tool (151). It was considered that lysine residues are more suitable than serine residues for immobilization of the protease for the reasons: a) unlike serine, lysine is not a catalytic residue of the protease, and any cross-linking reaction that involves lysine is, therefore, unlikely to negatively influence the catalytic activity of the enzyme, and b) there are six lysine residues located on the surface of the enzyme that could be targeted for immobilization of the protease on nanoparticles. The characterization of the support material and the enzyme-immobilized nanoparticles through various techniques, including FTIR spectroscopy, XRD analysis, DLS, and TGA, provides valuable insights into the structural and functional properties of the immobilized enzyme system.^{54–56} The FTIR analysis confirmed the successful immobilization of the subtilisin Carlsberg enzyme onto the Mag-CTS-GA-NPs, as evidenced by the detectable shifts in the characteristic peaks. FTIR is an analytical technique used for detection of functional groups and characterization of covalent bonding information. The spectral changes (shown in Figure 2) suggest strong evidence for the successful binding of subtilisin Carlsberg on to the (Mag-CTS-GA-NPs), indicating a potential approach for recovery and reusability of the enzyme.⁵⁷ XRD patterns indicated the presence of Fe_3O_4 nanoparticles in both the free and immobilized samples, while DLS revealed an increase in the average particle size upon enzyme immobilization, suggesting possible aggregation of the enzyme-immobilized particles. The XRD observation indicated that the resulting particles were pure Fe_3O_4 with a spinel structure. For enzyme immobilized magnetic nanoparticles (Mag-CTS-GA-Enz), the EDX analysis indicated an increase in the intensity of the peaks that were corresponding to carbon (C) and nitrogen (N) and was markedly higher compared to the (Mag-CTS-GA-NPs). The increase in the elemental composition of carbon (C) and nitrogen (N) in the enzyme immobilized nanoparticles clearly signifies the presence and inclusion of these elements within the sample, indicating a successful immobilization of the enzyme. The results found were in accordance with the study conducted for immobilization of HRP on magnetic nanoparticles using chitosan and glutaraldehyde as coating and cross-linking agents. Furthermore, the binding process

did not induce any major phase change in Fe_3O_4 particles.⁵⁸ The TGA analysis indicates a higher weight loss (approximately 30%) for enzyme immobilized nanoparticles compared to free nanoparticle (approximately 7%), confirming that enzyme immobilized nanoparticles exhibit a higher weight loss at elevated temperatures.⁵⁹

The kinetic parameters, such as the Michaelis–Menten constant (K_m) and maximum velocity (V_{\max}), provide valuable information about the catalytic efficiency and substrate affinity of enzymes.⁶⁰ The increase in K_m value upon immobilization suggests a reduced affinity of the immobilized enzyme for the substrate, which could be attributed to the diffusional limitations and steric hindrance imposed by the immobilization matrix.⁶¹ A similar increase in kinetic efficiency was reported for amylase immobilized on Fe_3O_4 nanoparticles, which exhibited a two-fold improvement in V_{\max} .⁶² However, the observed increase in V_{\max} indicates an enhancement in the catalytic efficiency of the immobilized enzyme, possibly due to increased enzyme stability and an altered microenvironment.⁶³ The immobilization yield, efficiency, and activity recovery are important parameters that assess the success of the immobilization process.⁶⁴ In this study, the immobilization yield of 61%, efficiency of 84%, and activity recovery of 50% demonstrate the effectiveness of the immobilization strategy in retaining a significant portion of the enzyme activity while providing the benefits of immobilization. In contrast, immobilized catalase on magnetic silica nanoparticles reported higher efficiency and activity recovery than subtilisin.⁶⁵ The slightly lower recovery for subtilisin could be due to the steric hindrance introduced by its larger molecular structure or the specific surface chemistry of the magnetic nanoparticles.⁶⁶

The stability studies of the immobilized and free enzyme under varying temperature and pH conditions confirmed the enhanced stability of the immobilized enzyme compared to its free counterpart. The immobilization of enzyme yield in higher activity retention across different conditions such 75% at 70°C and at a broader range of pH i.e. from 7 to 11. These results are consistent with previous data, that immobilization of enzymes help in improving stability under harsh conditions.⁶⁷ Similar trends have been reported for glucose oxidase immobilized on magnetic nanoparticles, where a 60% activity retention was observed at 60 °C.⁶⁸ This suggests that the chitosan-glutaraldehyde linkage effectively enhances thermal resilience, making subtilisin comparable or superior to other enzymes immobilized on magnetic supports. The enhancement in thermal stability is attributed to attachment of support material which help in stabilizing the enzymes tertiary structure.⁶⁹ The greater stability and reusability of enzymes are crucial in determining their industrial applicability and economic viability.⁴⁸ The immobilized of subtilisin Carlsberg enzyme resulted in improved storage stability which help in retaining approximately 53% of its activity after 30 days of storage at 4°C. In contrast the activity of free enzymes was dropped to 50%. This indicates significant improvement compared to the free enzyme, further strategies could be employed to enhance long-term stability. One potential approach is the incorporation of additional protective coatings or stabilizers, which have been shown to mitigate enzyme denaturation and leaching in immobilized systems.⁵⁴ The application of secondary polymer coatings such as polyethylene glycol (PEG) or silica could create a more robust protective layer around the enzyme, shielding it from environmental factors such as oxidation or hydrolysis.⁷⁰ PEGylation, in particular, is known to improve both thermal and storage stability by reducing enzyme flexibility and preventing aggregation. Alternatively, silica encapsulation could provide a rigid, biocompatible framework, further preserving the enzyme's active conformation.⁷¹ The reusability studies revealed that the immobilized enzyme retained 70% of its activity after 10 cycles of use. In comparison, immobilized lipase on Fe_3O_4 nanoparticles functionalized with polyethyleneimine, reported activity retention of up to 85% after 8 cycles.⁷² These findings highlight the potential of immobilization in extending the shelf life and operational stability of enzymes, thereby reducing the cost associated with enzyme replacement and process downtime.^{73,74} The enhanced stability, reusability, and catalytic efficiency of subtilisin Carlsberg immobilized on magnetic nanoparticles make it a promising candidate for integration into various industrial applications. The increased thermostability, as demonstrated by 75% activity retention at 70 °C compared to 50% for the free enzyme, aligns well with the diverse temperature requirements of industries such as detergent manufacturing, textile processing, and food production, where enzymes often operate under elevated temperatures.⁷⁵ However, to translate these findings into industrial applications, it is essential to evaluate the scalability of the immobilization process. The synthesis of magnetic nanoparticles is a critical step that needs optimization for large-scale production.⁷⁶ Methods such as co-precipitation, currently used in this study, are scalable but require modifications to ensure uniform particle size and functionalization.⁷⁷ Continuous-flow reactors or spray drying techniques could be employed to produce nanoparticles in bulk with consistent quality and cost efficiency. The glutaraldehyde-based surface

functionalization used in this study can be scaled by employing automated or semi-automated systems to coat nanoparticles with chitosan and crosslink the enzyme.⁷⁸ To minimize enzyme usage and maximize efficiency during scale-up, strategies such as optimizing enzyme-to-nanoparticle ratios and employing high-throughput immobilization setups could be adopted. A major factor in scaling up any process is cost-efficiency.⁷⁹ While magnetic nanoparticles provide significant advantages, their synthesis and functionalization can be cost-intensive. Utilizing cost-effective precursors for nanoparticle synthesis (eg, biosynthesis using plant or microbial extracts) and alternative cross-linking agents could reduce production costs without compromising performance.⁸⁰ In large-scale processes, magnetic nanoparticles must be separated efficiently from reaction mixtures. Industrial-scale magnetic separators, such as drum separators or magnetic filtration systems, can be integrated into production lines.⁸¹ Furthermore, reactor designs must ensure uniform mixing and mass transfer to optimize immobilized enzyme performance.⁸² Scaling up immobilization processes presents challenges, including maintaining enzyme activity during scale-up and ensuring reproducibility across batches. Addressing these issues requires collaboration between researchers and industry stakeholders to design processes that are not only efficient but also economically and environmentally sustainable.⁸³

The method utilized in this study, involving glutaraldehyde-linked chitosan-coated magnetic nanoparticles, balances efficiency with environmental considerations. Chitosan, a biodegradable and renewable biopolymer derived from chitin, serves as a sustainable coating material, reducing the reliance on non-renewable chemical supports. Its biodegradability minimizes long-term environmental burdens associated with disposal.⁸⁴ The immobilization process targets lysine residues on the enzyme surface due to their accessibility and non-involvement in catalytic activity. However, this specificity may limit the broader applicability of the method for enzymes with fewer surface lysine residues or for enzymes where lysine residues are critical to structural integrity. Although the immobilization yield (61%) and efficiency (84%) reported in this study are favorable, they are not optimal. Loss of activity during the immobilization process, reflected in the activity recovery of 51%, suggests that further optimization is required to reduce activity loss and enhance the functional utility of the immobilized enzyme. The present study demonstrated enhanced stability, activity, and reusability of subtilisin Carlsberg, there remains scope for improving the method's efficiency and cost-effectiveness. Several strategies could be explored in future studies to optimize the immobilization process: The use of glutaraldehyde as a cross-linking agent, while effective, may not be the most economical or environmentally friendly option. Investigating alternative cross-linkers, such as genipin or carbodiimides, could offer reduced costs and lower environmental impact while maintaining or enhancing immobilization efficiency. Key parameters such as pH, temperature, enzyme concentration, and nanoparticle surface functionalization could be systematically optimized to maximize immobilization yield and activity recovery. Response surface methodology (RSM) or design of experiments (DoE) could be employed to identify the optimal conditions. The use of alternative nanoparticle coatings, such as silica or polyethylene glycol (PEG), might enhance enzyme-nanoparticle interactions and improve immobilization efficiency. These modifications could also increase enzyme stability and reduce aggregation during the immobilization process. Developing methods to regenerate and reuse nanoparticles after enzyme deactivation could significantly lower costs. Exploring mild regeneration conditions to strip deactivated enzymes while preserving nanoparticle integrity would be a valuable area for further research.

Conclusion

The present study highlights the potential of enzyme immobilization in enhancing stability and reusability of subtilisin Carlsberg. Halophilic bacterial strain *Bacillus haynesii* was successfully isolated and characterized from local salt mines, and the gene encoding subtilisin Carlsberg was successfully cloned and expressed in *E. coli*. Subtilisin Carlsberg enzyme was immobilized on glutaraldehyde-linked chitosan-coated magnetic nanoparticles which resulted in enhanced thermal stability, broader pH tolerance, improved storage stability and reusability compared to the free enzyme. The functional and structural properties of free and immobilized enzymes were determined using different techniques, such as FTIR, XRD, TGA and DLS. The enhancement in kinetic parameter, immobilization yield, storage efficiency and activity recovery confirm the effectiveness of enzyme immobilization. These findings highlight the potential of immobilized enzymes in industrial applications, offering improved stability, reusability, and catalytic performance.

Acknowledgment

The authors extend their appreciation to Taif University, Saudi Arabia, for supporting this work through project number (TU-DSPP-2024-02). The authors also extend their acknowledgment to Higher Education Department, Peshawar for their financial support to the initial study of the project.

Author Contributions

All authors made a significant contribution to the work reported, whether that is in the conception, study design, execution, acquisition of data, analysis and interpretation, or in all these areas; took part in drafting, revising or critically reviewing the article; gave final approval of the version to be published; have agreed on the journal to which the article has been submitted; and agree to be accountable for all aspects of the work.

Funding

The authors extend their appreciation to Taif University, Saudi Arabia, for supporting this work through project number (TU-DSPP-2024-02).

Disclosure

The authors report no conflicts of interest in this work.

References

- Guan Z-B, Luo Q, Wang H-R, Chen Y, Liao X-R. Bacterial laccases: promising biological green tools for industrial applications. *Cell Mol Life Sci*. 2018;75:3569–3592. doi:10.1007/s00018-018-2883-z
- Zhang Y, He S, Simpson BK. Enzymes in food bioprocessing—novel food enzymes, applications, and related techniques. *Curr Opin Food Sci*. 2018;19:30–35. doi:10.1016/j.cofs.2017.12.007
- Chapman J, Ismail AE, Dinu CZ. Industrial applications of enzymes: recent advances, techniques, and outlooks. *Catalysts*. 2018;8:238. doi:10.3390/catal8060238
- Madhavan A, Sindhu R, Binod P, Sukumaran RK, Pandey A. Strategies for design of improved biocatalysts for industrial applications. *Bioresour Technol*. 2017;245:1304–1313. doi:10.1016/j.biortech.2017.05.031
- Adrio JL, Demain AL. Microbial enzymes: tools for biotechnological processes. *Biomolecules*. 2014;4:117–139. doi:10.3390/biom4010117
- Liu L, Yang H, Shin H-D, Li J, Du G, Chen J. Recent advances in recombinant protein expression by *Corynebacterium*, *Brevibacterium*, and *Streptomyces*: from transcription and translation regulation to secretion pathway selection. *Appl Microbiol Biotechnol*. 2013;97:9597–9608. doi:10.1007/s00253-013-5250-x
- Dunlap CA, Schisler DA, Perry EB, Connor N, Cohan FM, Rooney AP. *Bacillus swezeyi* sp. nov. and *Bacillus haynesii* sp. nov. isolated from desert soil. *Int J Syst Evol Microbiol*. 2017;67:2720–2725. doi:10.1099/ijsem.0.002007
- Gulmez C, Atakisi O, Dalgınlı KY, Atakisi E. A novel detergent additive: organic solvent- and thermo-alkaline-stable recombinant subtilisin. *Int J Biol Macromol*. 2018;108:436–443. doi:10.1016/j.ijbiomac.2017.11.133
- Aftab S, Ahmed S, Saeed S, Rasool SA. Screening, isolation and characterization of alkaline protease producing bacteria from soil. *Pak J Biol Sci*. 2006;9:2122–2126. doi:10.3923/pjbs.2006.2122.2126
- Abusham RA, Rahman RNZR, Salleh AB, Basri M. Optimization of physical factors affecting the production of thermo-stable organic solvent-tolerant protease from a newly isolated halo tolerant *Bacillus subtilis* strain Rand. *Microb Cell Fact*. 2009;8:1–9. doi:10.1186/1475-2859-8-20
- Sharma KM, Kumar R, Panwar S, Kumar A. Microbial alkaline proteases: optimization of production parameters and their properties. *J Genet Eng Biotechnol*. 2017;15:115–126. doi:10.1016/j.jgeb.2017.02.001
- Ikemura H, Inouye M. In vitro processing of pro-subtilisin produced in *Escherichia coli*. *J Biol Chem*. 1988;263:12959–12963. doi:10.1016/S0021-9258(18)37656-7
- Ohta Y, Hojo H, Aimoto S, et al. Pro-peptide as an intermolecular chaperone: renaturation of denatured subtilisin E with a synthetic pro-peptide. *Mol Microbiol*. 1991;5:1507–1510. doi:10.1111/j.1365-2958.1991.tb00797.x
- Ghasemi Y, Dabbagh F, Ghasemian A. Cloning of a fibrinolytic enzyme (subtilisin) gene from *Bacillus subtilis* in *Escherichia coli*. *Mol Biotechnol*. 2012;52:1–7. doi:10.1007/s12033-011-9467-6
- Bjerga GEK, Arsin H, Larsen Ø, Puntervoll P, Kleivdal HT. A rapid solubility-optimized screening procedure for recombinant subtilisins in *E. coli*. *J Biotechnol*. 2016;222:38–46. doi:10.1016/j.jbiotec.2016.02.009
- Mechri S, Jaouadi NZ, Bouacem K, et al. Cloning and heterologous expression of subtilisin SAPN, a serine alkaline protease from *Melghiribacillus thermohalophilus* Nari2AT in *Escherichia coli* and *Pichia pastoris*. *Process Biochem*. 2021;105:27–41. doi:10.1016/j.procbio.2021.03.020
- Seenuvasan M, Vinodhini G, Malar CG, Balaji N, Kumar KS. Magnetic nanoparticles: a versatile carrier for enzymes in bio-processing sectors. *IET Nanobiotechnol*. 2018;12:535–548. doi:10.1049/iet-nbt.2017.0041
- Monteiro RR, Lima PJ, Pinheiro BB, et al. Immobilization of lipase A from *Candida Antarctica* onto chitosan-coated magnetic nanoparticles. *Int J Mol Sci*. 2019;20:4018. doi:10.3390/ijms20164018
- Hosseiniipour SL, Khiabani MS, Hamishehkar H, Salehi R. Enhanced stability and catalytic activity of immobilized α -amylase on modified Fe₃O₄ nanoparticles for potential application in food industries. *J Nanopart Res*. 2015;17:1–13. doi:10.1007/s11051-015-3174-3

20. Husain Q. Nanocarriers immobilized proteases and their industrial applications: an overview. *J Nanosci Nanotechnol.* **2018**;18:486–499. doi:10.1166/jnn.2018.15246
21. Pakapongpan S, Poo-Arporn RP. Self-assembly of glucose oxidase on reduced graphene oxide-magnetic nanoparticles nanocomposite-based direct electrochemistry for reagentless glucose biosensor. *Mater Sci Eng C.* **2017**;76:398–405. doi:10.1016/j.msec.2017.03.031
22. Bilal M, Rasheed T, Iqbal HM, Yan Y. Peroxidases-assisted removal of environmentally-related hazardous pollutants with reference to the reaction mechanisms of industrial dyes. *Sci Total Environ.* **2018**;644:1–13. doi:10.1016/j.scitotenv.2018.06.274
23. Darwesh OM, Matter IA, Eida MF. Development of peroxidase enzyme immobilized magnetic nanoparticles for bioremediation of textile wastewater dye. *J Environ Chem Eng.* **2019**;7:102805. doi:10.1016/j.jece.2018.11.049
24. Xu J, Sun J, Wang Y, Sheng J, Wang F, Sun M. Application of iron magnetic nanoparticles in protein immobilization. *Molecules.* **2014**;19:11465–11486. doi:10.3390/molecules190811465
25. Han F, Sari N. Improvement of catalysis performance of pepsin and lipase enzymes by double enzyme immobilization method. *RSC Adv.* **2024**;14:11232–11243. doi:10.1039/D4RA00842A
26. Tercan Ç, Sürmeli Y, Şanlı-mohamed G. Thermoalkalophilic recombinant esterase entrapment in chitosan/calcium/alginate-blended beads and its characterization. *J Chem Technol Biotechnol.* **2021**;96:2257–2264. doi:10.1002/jctb.6750
27. Abdollahi N, Lavasani AS. Enzyme microencapsulation technique in food industry: a Review. *Int J Bio-Inorg Hybrid Nanomater.* **2021**;10:249–263.
28. Chen N, Chang B, Shi N, Yan W, Lu F, Liu F. Cross-linked enzyme aggregates immobilization: preparation, characterization, and applications. *Crit Rev Biotechnol.* **2023**;43:369–383. doi:10.1080/07388551.2022.2038073
29. Imam HT, Marr PC, Marr AC. Enzyme entrapment, biocatalyst immobilization without covalent attachment. *Green Chem.* **2021**;23:4980–5005. doi:10.1039/D1GC01852C
30. Özbek B, Ünal Ş. Preparation and characterization of polymer-coated mesoporous silica nanoparticles and their application in Subtilisin immobilization. *Korean J Chem Eng.* **2017**;34:1992–2001. doi:10.1007/s11814-017-0045-x
31. Rodrigues RC, Hernandez K, Barbosa O, et al. Immobilization of proteins in poly-styrene-divinylbenzene matrices: functional properties and applications. *Curr Org Chem.* **2015**;19:1707–1718. doi:10.2174/1385272819666150429231728
32. Zahirinejad S, Hemmati R, Homaei A, et al. Nano-organic supports for enzyme immobilization: scopes and perspectives. *Colloids Surf B.* **2021**;204:111774. doi:10.1016/j.colsurfb.2021.111774
33. Yang A, Long C, Xia J, et al. Enzymatic characterisation of the immobilised Alcalase to hydrolyse egg white protein for potential allergenicity reduction. *J Sci Food Agric.* **2017**;97(1):199–206. doi:10.1002/jsfa.7712
34. Zdarta J, Meyer AS, Jesionowski T, Pinelo M. A general overview of support materials for enzyme immobilization: characteristics, properties, practical utility. *Catalysts.* **2018**;8:92. doi:10.3390/catal8020092
35. Yazid NA, Barrena R, Sánchez A. The immobilisation of proteases produced by SSF onto functionalized magnetic nanoparticles: application in the hydrolysis of different protein sources. *J Mol Catal B Enzym.* **2016**;133:S230–S242. doi:10.1016/j.molcatb.2017.01.009
36. Eser A, Aydemir T. Subtilisin Carlsberg immobilization and its application for eco-friendly leather processing. *J Cleaner Prod.* **2022**;377:134296. doi:10.1016/j.jclepro.2022.134296
37. Kikani B, Patel R, Thumar J, et al. Solvent tolerant enzymes in extremophiles: adaptations and applications. *Int J Biol Macromol.* **2023**;238:124051. doi:10.1016/j.ijbiomac.2023.124051
38. Kochhar N, Shrivastava S, Ghosh A, Rawat VS, Sodhi KK, Kumar M. Perspectives on the microorganism of extreme environments and their applications. *Curr Res Microb Sci.* **2022**;3:100134. doi:10.1016/j.crmicr.2022.100134
39. Masi C, Tebiso A, Kumar KS. Isolation and characterization of potential multiple extracellular enzyme-producing bacteria from waste dumping area in Addis Ababa. *Heliyon.* **2023**;9:e12645. doi:10.1016/j.heliyon.2022.e12645
40. Verma S, Kumar R, Kumar P, et al. Cloning, characterization, and structural modeling of an extremophilic bacterial lipase isolated from saline habitats of the Thar desert. *Appl Biochem Biotechnol.* **2020**;192:557–572. doi:10.1007/s12010-020-03329-3
41. Solanki P, Putatunda C, Kumar A, Bhatia R, Walia A. Microbial proteases: ubiquitous enzymes with innumerable uses. *3 Biotech.* **2021**;11:428. doi:10.1007/s13205-021-02928-z
42. Tavanti M. Synthetic DNA libraries for protein engineering toward process improvement in drug synthesis. In: *Enzyme Engineering: Methods and Protocols.* Springer; **2021**:33–45.
43. Lozano Terol G, Gallego-Jara J, Sola Martinez RA, Martinez Vivancos A, Canovas Diaz M, de Diego Puente T. Impact of the expression system on recombinant protein production in Escherichia coli BL21. *Front Microbiol.* **2021**;12:682001. doi:10.3389/fmicb.2021.682001
44. Rana AM, Devreese B, De Waele S, et al. Immobilization and docking studies of Carlsberg subtilisin for application in poultry industry. *PLoS One.* **2023**;18:e0269717. doi:10.1371/journal.pone.0269717
45. Webb B, Sali A. *Protein Structure Modeling With MODELLER.* Springer; **2021**.
46. Zheng Z-L, Zuo Z-Y, Liu Z-G, Tsai K-C, Liu A-F, Zou G-L. Construction of a 3D model of nattokinase, a novel fibrinolytic enzyme from Bacillus natto: a novel nucleophilic catalytic mechanism for nattokinase. *J mol Graphics Modell.* **2005**;23:373–380. doi:10.1016/j.jmgm.2004.10.002
47. Ashkan Z, Hemmati R, Homaei A, Dinari A, Jamlidoost M, Tashakor A. Immobilization of enzymes on nanoorganic support materials: an update. *Int J Biol Macromol.* **2021**;168:708–721. doi:10.1016/j.ijbiomac.2020.11.127
48. Mariño MA, Fulaz S, Tasic L. Magnetic nanomaterials as biocatalyst carriers for biomass processing: immobilization strategies, reusability, and applications. *Magnetochemistry.* **2021**;7:133. doi:10.3390/magnetochemistry7100133
49. Bilal M, Iqbal HM. Chemical, physical, and biological coordination: an interplay between materials and enzymes as potential platforms for immobilization. *Coord Chem Rev.* **2019**;388:1–23. doi:10.1016/j.ccr.2019.02.024
50. Jesionowski T, Zdarta J, Krajewska B. Enzyme immobilization by adsorption: a review. *Adsorption.* **2014**;20:801–821. doi:10.1007/s10450-014-9623-y
51. Liu ZM, Becker T, Neufeld RJ. Spherical Alginate Granules formulated for quick-release active Subtilisin. *Biotechnol Progr.* **2005**;21:568–574. doi:10.1021/bp049736g
52. Rossi LM, Costa NJ, Silva FP, Wojcieszak R. Magnetic nanomaterials in catalysis: advanced catalysts for magnetic separation and beyond. *Green Chem.* **2014**;16:2906–2933. doi:10.1039/c4gc00164h

53. Liu D-M, Chen J, Shi Y-P. Advances on methods and easy separated support materials for enzymes immobilization. *TrAC Trends Anal Chem.* **2018**;102:332–342. doi:10.1016/j.trac.2018.03.011
54. Aggarwal S, Chakravarty A, Ikram S. A comprehensive review on incredible renewable carriers as promising platforms for enzyme immobilization & thereof strategies. *Int J Biol Macromol.* **2021**;167:962–986. doi:10.1016/j.ijbiomac.2020.11.052
55. Pekdemir SS, Bakar B, Taş R, Ulu A, Pekdemir ME, Ateş B. Immobilization of Xylanase on ZnO nanoparticles obtained by green synthesis from *Eupatorium cannabinum* L. and its application in enrichment of fruit juices. *Mol Catal.* **2024**;562:114232. doi:10.1016/j.mcat.2024.114232
56. Murugappan G, Khambhay Y, Sreeram KJ. Protease immobilized nanoparticles: a cleaner and sustainable approach to dehairing of skin. *Appl Nanosci.* **2020**;10:213–221. doi:10.1007/s13204-019-01113-2
57. Bilal M, Qamar SA, Carballares D, Berenguer-Murcia Á, Fernandez-Lafuente R. Proteases immobilized on nanomaterials for biocatalytic, environmental and biomedical applications: advantages and drawbacks. *Biotechnol Adv* **2023**;108304. doi:10.1016/j.biotechadv.2023.108304
58. Hwang ET, Lee B, Zhang M, et al. Immobilization and stabilization of subtilisin Carlsberg in magnetically-separable mesoporous silica for transesterification in an organic solvent. *Green Chem.* **2012**;14:1884–1887. doi:10.1039/c2gc35559k
59. Hosseini SH, Hosseini SA, Zohreh N, Yaghoobi M, Pourjavadi A. Covalent immobilization of cellulase using magnetic poly (ionic liquid) support: improvement of the enzyme activity and stability. *J Agric Food Chem.* **2018**;66:789–798. doi:10.1021/acs.jafc.7b03922
60. Carrillo N, Ceccarelli EA, Roveri OA. Usefulness of kinetic enzyme parameters in biotechnological practice. *Biotechnol Genet Eng Rev.* **2010**;27:367–382. doi:10.1080/02648725.2010.10648157
61. Pal A, Khanum F. Covalent immobilization of xylanase on glutaraldehyde activated alginate beads using response surface methodology: characterization of immobilized enzyme. *Process Biochem.* **2011**;46:1315–1322. doi:10.1016/j.procbio.2011.02.024
62. Sohrabi N, Rasouli N, Torkzadeh M. Enhanced stability and catalytic activity of immobilized α -amylase on modified Fe₃O₄ nanoparticles. *Chem Eng J.* **2014**;240:426–433. doi:10.1016/j.cej.2013.11.059
63. Bilal M, Zhao Y, Noreen S, Shah SZH, Bharagava RN, Iqbal HM. Modifying bio-catalytic properties of enzymes for efficient biocatalysis: a review from immobilization strategies viewpoint. *Biocatal Biotransform.* **2019**;37:159–182. doi:10.1080/10242422.2018.1564744
64. Cantone S, Ferrario V, Corici L, et al. Efficient immobilisation of industrial biocatalysts: criteria and constraints for the selection of organic polymeric carriers and immobilisation methods. *Chem Soc Rev.* **2013**;42:6262–6276. doi:10.1039/c3cs35464d
65. Jayathilaka HA. Catalase immobilization in Wrinkled mesoporous silica nanoparticles **2018**.
66. DePaz RA, Dale DA, Barnett CC, Carpenter JF, Gaertner AL, Randolph TW. Effects of drying methods and additives on the structure, function, and storage stability of subtilisin: role of protein conformation and molecular mobility. *Enzyme Microb Technol.* **2002**;31:765–774. doi:10.1016/S0141-0229(02)00173-4
67. Rodrigues RC, Berenguer-Murcia Á, Fernandez-Lafuente R. Coupling chemical modification and immobilization to improve the catalytic performance of enzymes. *Adv Synth Catal.* **2011**;353:2216–2238. doi:10.1002/adsc.201100163
68. Abbasi M, Amiri R, Bordbar A-K, Ranjbakhsh E, Khosropour A-R. Improvement of the stability and activity of immobilized glucose oxidase on modified iron oxide magnetic nanoparticles. *Appl Surf Sci.* **2016**;364:752–757. doi:10.1016/j.apsusc.2015.12.120
69. Guisan JM, Fernandez-Lorente G, Rocha-Martin J, Moreno-Gamero D. Enzyme immobilization strategies for the design of robust and efficient biocatalysts. *Curr Opin Green Sustainable Chem.* **2022**;35:100593. doi:10.1016/j.cogsc.2022.100593
70. Kumar AP, Depan D, Tomer NS, Singh RP. Nanoscale particles for polymer degradation and stabilization—trends and future perspectives. *Prog Polym Sci.* **2009**;34:479–515. doi:10.1016/j.progpolymsci.2009.01.002
71. Shi M, McHugh KJ. Strategies for overcoming protein and peptide instability in biodegradable drug delivery systems. *Adv Drug Delivery Rev.* **2023**;199:114904. doi:10.1016/j.addr.2023.114904
72. Perçin I, Tamahkar E, Idil N, Bayrak G, Aslıyüce S, Denizli A. Functionalized magnetic nanosystems for immobilization of proteins and enzymes. In: *Functionalized Magnetic Nanosystems for Diagnostic Tools and Devices*. Elsevier; **2024**:291–326.
73. Taheri-Kafrani A, Kharazmi S, Nasrollahzadeh M, et al. Recent developments in enzyme immobilization technology for high-throughput processing in food industries. *Crit Rev Food Sci Nutr.* **2021**;61:3160–3196. doi:10.1080/10408398.2020.1793726
74. Valerio SG, Alves JS, Klein MP, Rodrigues RC, hertz PF. High operational stability of invertase from *Saccharomyces cerevisiae* immobilized on chitosan nanoparticles. *Carbohydr Polym.* **2013**;92:462–468. doi:10.1016/j.carbpol.2012.09.001
75. Rai SK, Mukherjee AK. Statistical optimization of production, purification and industrial application of a laundry detergent and organic solvent-stable subtilisin-like serine protease (Alzwitterase) from *Bacillus subtilis* DM-04. *Biochem Eng J.* **2010**;48:173–180. doi:10.1016/j.bej.2009.09.007
76. Cavalcante ALG, Dari DN, da Silva Aires FI, de Castro EC, Dos Santos KM, Dos Santos JCS. Advancements in enzyme immobilization on magnetic nanomaterials: toward sustainable industrial applications. *RSC Adv.* **2024**;14:17946–17988. doi:10.1039/d4ra02939a
77. García-Merino B, Bringas E, Ortiz I. Synthesis and applications of surface-modified magnetic nanoparticles: progress and future prospects. *Rev Chem Eng.* **2022**;38:821–842. doi:10.1515/revce-2020-0072
78. Garzon-Tovar L, Cano-Sarabia M, Carné-Sánchez A, Carbonell C, Imaz I, Maspocho D. A spray-drying continuous-flow method for simultaneous synthesis and shaping of microspherical high nuclearity MOF beads. *React Chem Eng.* **2016**;1:533–539. doi:10.1039/C6RE00065G
79. Premaratne G, Nerimetla R, Matlock R, et al. Stability, scalability, and reusability of a volume efficient biocatalytic system constructed on magnetic nanoparticles. *Catal Sci Technol.* **2016**;6:2361–2369. doi:10.1039/C5CY01458A
80. García PF, Brammen M, Wolf M, Reinlein S, Von Roman MF, Berensmeier S. High-gradient magnetic separation for technical scale protein recovery using low cost magnetic nanoparticles. *Sep Purif Technol.* **2015**;150:29–36. doi:10.1016/j.seppur.2015.06.024
81. Hutchins DL. *Continuous Flow Process for Recovery of Metal Contaminants From Industrial Wastewaters With Magnetic Nanocomposites*. Montana Tech of The University of Montana; **2018**.
82. de Lathouder KM, Bakker J, Kreutzer MT, Kapteijn F, Moulijn JA, Wallin SA. Structured reactors for enzyme immobilization: advantages of tuning the wall morphology. *Chem Eng Sci.* **2004**;59:5027–5033. doi:10.1016/j.ces.2004.07.047
83. Bolívar JM, Woodley JM, Fernandez-Lafuente R. Is enzyme immobilization a mature discipline? Some critical considerations to capitalize on the benefits of immobilization. *Chem Soc Rev.* **2022**;51:6251–6290. doi:10.1039/d2cs00083k
84. Chincholikar P, Singh KR, Natarajan A, et al. Green nanobiopolymers for ecological applications: a step towards a sustainable environment. *RSC Adv.* **2023**;13:12411–12429. doi:10.1039/D2RA07707H

Nanotechnology, Science and Applications**Dovepress**
Taylor & Francis Group**Publish your work in this journal**

Nanotechnology, Science and Applications is an international, peer-reviewed, open access journal that focuses on the science of nanotechnology in a wide range of industrial and academic applications. It is characterized by the rapid reporting across all sectors, including engineering, optics, bio-medicine, cosmetics, textiles, resource sustainability and science. Applied research into nano-materials, particles, nano-structures and fabrication, diagnostics and analytics, drug delivery and toxicology constitute the primary direction of the journal. The manuscript management system is completely online and includes a very quick and fair peer-review system, which is all easy to use. Visit <http://www.dovepress.com/testimonials.php> to read real quotes from published authors.

Submit your manuscript here: <https://www.dovepress.com/nanotechnology-science-and-applications-journal>